NOTE

Assembly of cell-laden hydrogel fiber into non-liquefied and liquefied 3D spiral constructs by perfusion-based layer-by-layer technique

Biofabrication

RECEIVED
11 September 2014

ACCEPTED FOR PUBLICATION
11 December 2014

PUBLISHED
6 January 2015

NOTE

Assembly of cell-laden hydrogel fiber into non-liquefied and liquefied 3D spiral constructs by perfusion-based layer-by-layer technique

Praveen Sher[1,2], **Sara M Oliveira**[1,2], **João Borges**[1,2] **and João F Mano**[1,2]

[1] 3B's Research Group—Biomaterials, Biodegradables and Biomimetics, University of Minho, Headquarters of the European Institute of Excellence of Tissue Engineering and Regenerative Medicine, AvePark, Zona Industrial da Gandra, S. Cláudio do Barco, 4806-909 Caldas das Taipas—Guimarães, Portugal

[2] ICVS/3B's, PT Government Associated Laboratory, Braga/Guimarães, Portugal

E-mail: sherpraveen@gmail.com, praveen.sher@dep.uminho.pt **and** jmano@dep.uminho.pt

Keywords: cell-encapsulation, hydrogel fiber, chelation, layer-by-layer, switching cell microenviroment, liquefied core, tissue engineering

Supplementary material for this article is available online

Abstract

In this work, three-dimensional (3D) self-sustaining, spiral-shaped constructs were produced through a combination of ionotropic gelation, to form cell-encapsulated alginate fibers, and a perfusion-based layer-by-layer (LbL) technique. Single fibers were assembled over cylindrical molds by reeling to form spiral shapes, both having different geometries and sizes. An uninterrupted nanometric multilayer coating produced by a perfusion-based LbL technique, using alginate and chitosan, generated stable 3D spiral-shaped macrostructures by gripping and affixing the threads together without using any crosslinking/binding agent. The chelation process altered the internal microenvironment of the 3D construct from the solid to the liquefied state while preserving the external geometry. L929 cell viability by MTS and dsDNA quantification favor liquefied 3D constructs more than non-liquefied ones. The proposed technique setup helps us to generate complex polyelectrolyte-based 3D constructs for tissue engineering applications and organ printing.

1. Introduction

Tissue engineering (TE) strategies have been concerned with the development of functional and complex constructs aiming for the full replacement, restoration, and/or regeneration of defective or injured functional living tissues and organs. In recent decades, bottom-up approaches have raised considerable interest in the development of complex, larger, and functional three-dimensional (3D) tissue-like structures for TE through the assembly of smaller building blocks [1–3]. The main aim of such structures is to mimic the hierarchical organization, complex composition, architecture, and functional behavior of native tissues along with the strategies that control the building blocks' properties over multiscale lengths [4–7]. Based on different shapes of building blocks, cell-laden fibers/tubes show promising applications in the field of TE, owing to their great potential to generate and replicate a wide variety of complex tubular structures, such as urethra, trachea, or esophagus. These structures, which are either polymeric or synthetic, hollow or closed, range from millimeter- to the centimeter-length scales such as blood vessels, neural pathways, and muscle fibers. They have been designed and engineered in two steps: firstly by producing fibers or tubes and then by their assembly, using different methods with cell-seeding options, either from the start or afterward, depending on the fabrication process. Common approaches to fabricate such structures are electro-, wet-, melt-, or microfluidic-spinning techniques [8–11]. As for the assembling methods, random fiber deposition, weaving, knitting, and braiding have been used to produce the final 3D structure [12–18]. Besides the aforementioned methods, other works have reported the use of bioprinting techniques, including extrusion printing, lithography/direct writing, or stereolithography to generate such 3D structures [19–22]. However, the majority of these technologies entail distinctive

working conditions in the form of sophisticated and expensive equipment or require the usage of not so cell-friendly conditions such as organic solvents, high temperatures, or crosslinking agents. Though necessary and cytocompatible, they can be potentially undesirable for bioactive molecules and living cells [23]. Moreover, these engineered structures often lack some desired traits, namely, modulation of the internal cell microenvironment, which is mostly of a solid/elastic nature and, if altered, could display better cell behavior [24, 25]. As a stimulating alternative, it would be worthwhile to have a biofabrication process that will not only provide facilitation and flexibility in modulating or enhancing fiber-based external architecture but also provide an option to switch the internal cell microenvironment from a solid/elastic matrix to a liquefied environment, without affecting the construct shape.

Pursuing the aforementioned aims, herein we propose a methodology for the development of 3D spiral-shaped, cell-laden hydrogel constructs through the combination of ionotropic gelation and a perfusion-based layer-by-layer (LbL) technique. This approach can offer distinct advantages for using fibers as building blocks for TE strategies.

2. Material and methods

2.1. Material

Water-soluble polyelectrolytes were selected for this work: chitosan (Protasan UP CL 213, viscosity 107 mPa s, NovaMatrix, Norway) and low-viscosity alginate from brown algae (250 cP, SigmaAldrich, USA). Sodium chloride (NaCl, Panreac, Spain), glacial acetic acid (CH_3COOH, Panreac, Spain), sodium hydroxide (NaOH, Panreac Spain), calcium chloride ($CaCl_2$, Merck, Germany), ethylenediaminetetraacetic acid (EDTA, Sigma-Aldrich, USA) were used as received.

2.2. Assembly of alginate fibers to fabricate 3D spiral construct

The solid alginate fibers were generated by a simple ionotropic gelation method using 0.5 mL of alginate solution at a concentration of 1.2% w/v. A fixed amount of solution volume was primarily used to maintain the uniformity between fibers. The pH of the alginate solution was adjusted to 7.0. Fibers were produced by extruding the alginate solution through a syringe with a 21 G needle directly inside of $_a$ 0.1 M $CaCl_2$ solution and kept there for 20 min. Then, the Ca-Alg fibers were collected and rinsed with 0.15 M NaCl.

A cylindrical glass rod was used to manually reel/weave single alginate fibers over it, transforming it in the 3D template with a spiral shape. Afterward, this glass rod was carefully taken out while transferring the wound-up fiber over the perforated plate simply by pressing it in the opposite direction. This was followed by performing perfusion-based LbL, which is based on the sequential drop-wise method of complementary polyelectrolyte solutions, as reported already [29–31]. Solutions of Cht and Alg with a concentration of 1 mg mL^{-1} were used to coat over this weaved 3D template until five bilayers were assembled to form a 3D spiral construct. Intermediate rinsing steps were performed using 0.15 M NaCl aqueous solutions. All solutions were adjusted to pH 7.0.

After the formation of the 3D spiral construct, a liquefaction process was performed by immersing it in 0.05 M EDTA at pH 7.0 for 7 min. The obtained non-liquefied constructs were then rinsed with a 0.15 M NaCl aqueous solution.

2.3. Cell culture

Cell studies were performed using L929 cells, the murine fibrosarcoma cell line obtained from the European Collection of Cell Cultures. Cells were grown in Dulbecco's Modified Eagle's medium-low glucose (DMEM, Sigma-Aldrich) with phenol red and supplemented with 10% heat-inactivated fetal bovine serum (FBS, Alfagene) and 1% antibiotic-antimycotic solution (AT, Alfagene) in a humidified atmosphere with 5% CO_2 at 37 °C. For expansion, confluent cell cultures were split into a ratio of 1/3 to 1/6 using TrypLE™ Express. L929 cells were used in passages between 16 and 36. To proceed with the cell seeding, cells were harvested by trypsinization and filtered with a cell strainer with a pore size of 100 microns to remove possible cell aggregates. A concentration of 0.5 million cells per mL was used for cell encapsulation, and all the samples were prepared with 0.5 mL of this alginate/cells re-suspension. After finishing the procedure, the constructs were completely immersed in approximately 4 ml of medium and cultured for 7 d in a humidified atmosphere with 5% CO_2 at 37 °C. The medium surrounding the constructs was exchanged every three days.

2.4. LIVE/DEAD assay

LIVE/DEAD assay is used to measure cell viability. It is a two-color fluorescence assay that simultaneously highlights the living (green) and dead (red) cells. Briefly, the culture medium was removed and the samples washed twice with sterile PBS for 5 min. Then 250 μL of calcein AM solution and propidium iodide/RNAse solution were added and samples allowed to incubate for 10 min in the incubator, protected from light, after 7 d in culture. Then, the solutions were removed and samples washed twice with sterile PBS and observed under a transmitted reflected microscope using the red and green fluorescence filters.

2.5. dsDNA quantification

Proliferation quantification was done by computing dsDN, after 7 d of culture, via Quant-iT™ PicoGreen®

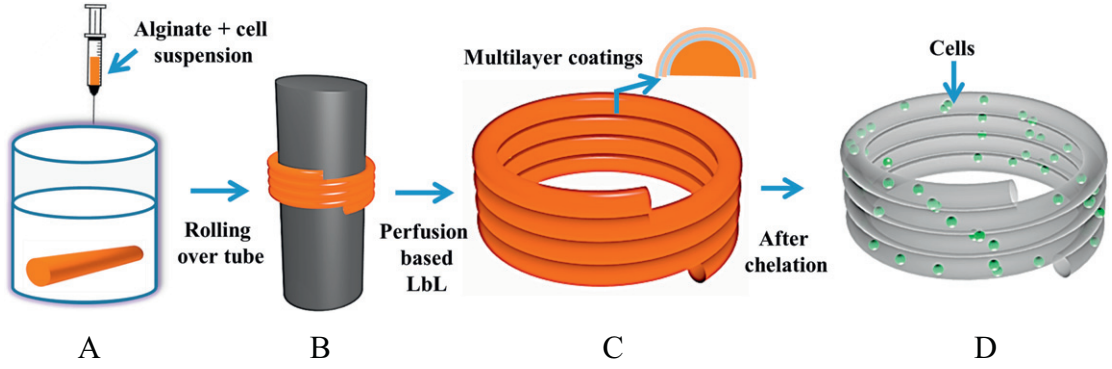

Scheme 1. Schematic illustration of the process to fabricate liquefied 3D helical structures using cell-encapsulated hydrogel fibers. (A) Cells are encapsulated in alginate hydrogel fibers by ionotropic gelation. (B) The fibers are reeled over the glass rod to form the spiral structure. (C) After removal of the glass rod and coating with five bilayers of Cht/Alg multilayers, spiral-shaped 3D constructs are obtained. This intermediate product can be referred to as a non-liquefied construct. (D) Liquefied 3D construct obtained after the chelation process. The difference in color indicates the liquefaction of the alginate solid core.

dsDNA assay kit (Molecular Probes/Invitrogen), which measures the amount of fluorescence produced by the excitation of UV light of PicoGreen dye while it attaches to dsDNA. The stepwise procedure included keeping samples for incubation and rinsing (thrice) with sterile PBS. This was followed by the addition of 1 mL of ultra-pure sterile, which was then kept at −80 °C until quantification. The quantification process started with samples being defrosted at room temperature and then sonicated. Also, 100 mL of Tris–EDTA buffer were transferred into a 96-well plate. The exact quantity of 28.8 μL of the sample, after being vortexed, was added to 71.2 μL of PicoGreen solution. A microplate reader using an excitation wavelength of 485 nm and emission wavelength of 528 nm was used to read the plate after 10 min of incubation in dark. Previously, a standard curve of dsDNA was done, using a concentration range of 0–2 mg mL^{-1}, to measure the values of dsDNA (triplicate). Overall, six specimens were measured for each sample. The experiment was repeated once.

2.6. MTS quantification

To measure cell viability, 96®AQ$_{ueous}$ One Solution Cell Proliferation assay (Promega, USA) was used that is based on the chemical bioreduction process of (3-(4,5-dimethylthiazol-2-yl)-5-(3-carboxymethoxy-phenyl)-2(4-sulfophenyl)-2 H tetrazolium) (MTS), which, when turned into a brown formazan product by dehy-drogenase enzymes, is an indicator of living cells. New wells were used to place samples that were previously rinsed twice in sterile PBS. 0.5 mL of culture medium, followed by the addition of MTS (5:1 ratio) without phenol red and FBS and further incubated for 3 h at 37 °C in 5% CO_2 atmosphere. After the incubation period, 100 μL was transferred to a 96-well plate (triplicate) to measure their absorbance at 490 nm by a microplate reader (Bio-Tek Synergie HT, USA).

2.7. Statistical analysis

All dsDNA and MTS data were statistically analyzed by using a non-parametric test as the Shapiro–Wilk test, which indicated that data did not have a normal distribution. The Kruskal–Wallis test was performed, considering $p < 0.05$ ($24 > n > 3$). The Dunn's test was used as a post-hoc test.

3. Results and discussion

Scheme 1 shows a schematic illustration of the overall biofabrication process. Briefly, cell-encapsulated alginate (Alg) hydrogel fibers (scheme 1(A)), made by ionotropic gelation with calcium ions, were manually aligned and reeled over a glass rod, acting as a cylindrical mold, in order to form a closely packed 3D helical fiber structure (scheme 1(B)). Then, these 3D structures were stabilized and linked by coating them with 5 bilayers of chitosan/alginate (Cht/Alg) multilayers through the perfusion-based LbL technique (scheme 1(C)). The intermediate generated structures were further processed by a chelation process, thus leading to liquefied 3D helical structures (scheme 1(D)) sustained solely by the assembled multilayers, which maintain the original 3D structure.

By adopting such a strategy, we merged the facile method of cell encapsulation process by ionotropic gelation [26–28] with the recently reported perfusion-based LbL approach [29–31]. Traditionally this combination, using conventional LbL deposition techniques like the dip-coating method, produces nanocoatings over cell-encapsulated hydrogel spheres with solid cores that, after the chelation process, are transformed into polyelectrolyte multilayered capsules with liquid cores [32–34]. The perfusion-based LbL technique, which differs from conventional LbL methods by the drop-wise addition of polyelectrolyte solutions, simultaneously provides coating and binding potential of nanometric multilayers in real time

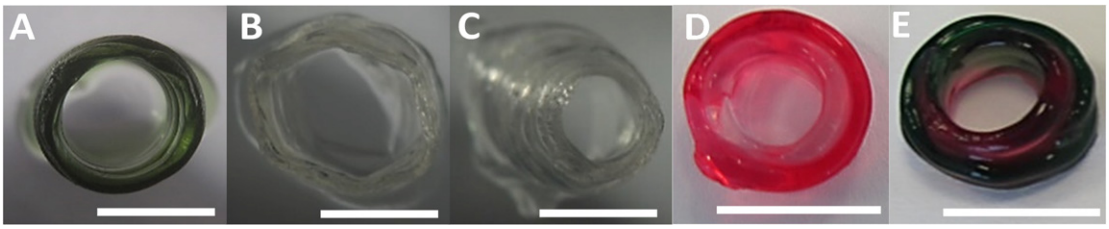

Figure 1. 3D helical Ca-Alg core constructs displaying easy modulation into different shapes and sizes obtained after the perfusion-based LbL technique. Top view of 3D core structures using single-fiber and different molds at higher magnifications. (A) Cylindrical mold, (B) hexagonal mold, and (C) spiral mold. (D), (E) complex tuning of the construct using two tubes sidewise to each other over a cylindrical mold. Food color dyes were used to obtain contrast and distinguish between two fibers. Scale bars: 1 cm.

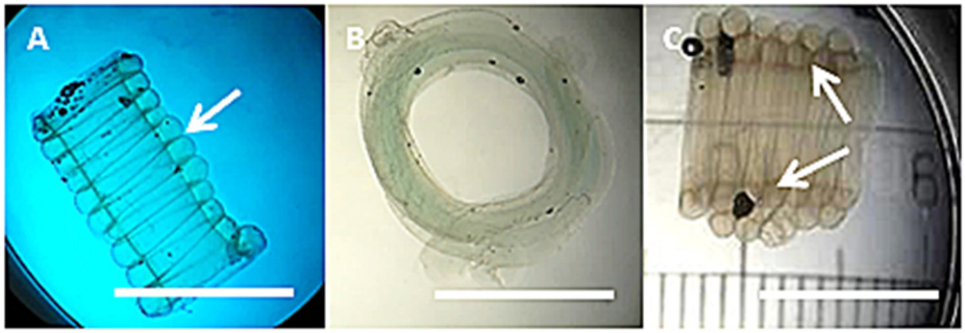

Figure 2. Optical images of the 3D construct after the liquefaction process by immersing in 0.05 M EDTA solution for 7 min. (A) Side view of the construct made of single-hydrogel fiber. The arrow indicates the single winding points all over the construct. (B) Top view of the 3D construct made of single-hydrogel fibers. (C) Side view of the 3D construct made of double-hydrogel fibers. The arrows indicate two winding points all over the construct. Scale bars: 1 cm.

[29–31]. This process allowed us to assemble, pattern, hold, and attach sacrificial paraffin sphere templates, placed over a perforated base, without using harsh processing conditions such as crosslinkers/binders or molds to produce organized porous 3D macrostructures entirely made of nanometric multilayers. This binding/sticking feature adds versatility to the LbL methodology by the holding and patterning of free-form spherical templates that primarily stick together into a delicate 3D core and unite during the multilayered process. This is an important feature of the perfusion-based LbL technique that excludes the stage of prefabricating strong 3D core objects as intrinsically necessary for conventional LbL methodologies [35, 36].

To verify the versatility of the proposed methodology, initial work was performed in which alginate-based solid fiber structures with different diameters were prepared by ionotropic gelation using a calcium ion bath (herein referred to as Ca-Alg) without cells. Then, the fibers were manually reeled over cylindrical molds with different diameters and external geometries to endow them with a spiral shape. These fibers showed excellent handling capacity, thus allowing winding without breaking. To increase the complexity, two fibers were weaved, one over the other, with the aim of using different materials together or even co-cultures. These spiral-shaped constructs were gently pushed over while carefully removing the cylindrical mold in the opposite direction and directly placing them over a perforated base. It must be noted that at this stage, these 3D spiral structures will easily disintegrate if moved. This was followed by the deposition of five bilayers of Cht and Alg by alternatively perfusing their solutions while intercalated by washing steps. The LbL coating not only stabilized and linked the initial fragile structure but also gave rise to a self-supporting multilayer-coated 3D spiral macrostructure. Figure 1 shows some optical images of the final 3D structures with different sizes and shapes, illustrating the versatility of this technique. (More pictures are enclosed in the supporting information.)

Throughout the perfusion-based LbL process, all 3D assemblies remained intact while maintaining the initial conformation. After this process was completed, the constructs were easily handled without disrupting their integrity. In order to show the formation, robustness, and effective binding capacity provided by the multilayer coating, the Ca-Alg 3D tubular structures were subjected to liquefaction by immersing them in EDTA solutions (figure 2). Optical pictures show the formation of the multilayer coating over the exposed fiber curves, as well as the contact areas within the whole construct, while also displaying increased transparency. Single- and double-reeled spiral constructs demonstrated the same results as seen in

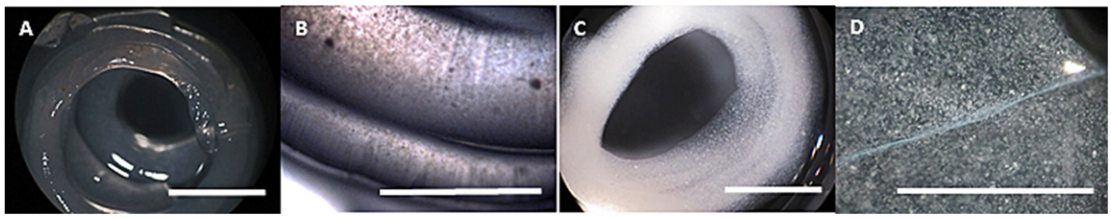

Figure 3. Optical images of the cell-encapsulated 3D constructs after 7 d of culture. (A) Top view of the construct after the LbL assembly process (non-liquefied). (B) Side view of (A) showing fibers winding over each other. (C) Top view of the liquefied 3D construct. (D) Clear multilayer binding of cell-encapsulated fibers at the thread between fiber structures after liquefaction. Scale bars: 5 mm.

figures 2(A)–(C), respectively. At this stage, it is important to highlight that these liquefied constructs displayed fair self-sustaining structural integrity. Contrary to their frail appearance, they showed good mechanical features that enabled us to easily control their handling during and after the fabrication process without unwinding or piercing, and, more importantly, they could maintain their initial configuration. These interpretations further validate the formation of steady and unbroken multilayer coatings throughout the whole construct, covering both external and internal surface outlines/contours. It is noteworthy to mention that this type of biofabrication, based on polyelectrolyte multilayers, can be performed only using the perfusion-based LbL technique, which clearly nullifies the interference or use of permanent molds that could otherwise be used to hold their shape and thereby interact with the multilayer processing. In this work, the use of molds was restricted to the initial 3D assembly/reeling of fibers that held their shape on their own to be ready for the multilayer process. These results not only validate the process but also demonstrate the suitability of the perfusion-based LbL technique to produce liquefied 3D spiral constructs using hydrogel fibers as building blocks.

In the context of the present work, this approach provides stimulating advantages over the current existing LbL deposition methods [32–36] and other methodologies [6–22], since it does not require strong intermediate 3D core structures, potentially toxic denaturizing crosslinking agents, UV-visible light, or high temperatures during the fabrication process. In addition, the proposed methodology significantly reduces the time and amount of polyelectrolyte solutions needed for the deposition process, thus surpassing some of the limitations of the dip-coating LbL method. Furthermore, this fabrication process can be easily conducted on the bench top, thus making it cost-effective and more environmentally friendly.

Moreover, the production of these constructs using this simple process quite resembles those obtained from other approaches based on microfluidics, while using reeling over the tube or a laser printing technique [7–18].The manual plain weaving of the alginate fibers was easy to handle, which can be more advantageous than using thin fibers that can get entangled or damaged during this process. Another important advantage includes switching to a liquefied state without affecting the external shape, thus the possibility of engineering hydrogel matrices by incorporating analogues or biologically relevant physicochemical cues for cell growth.

At this stage, we intended to extend and demonstrate the feasibility of the proposed methodology to fabricate Ca-Alg hydrogel fibers encapsulating L929 fibroblast-like cells, with the aim of producing higher-order cellular assembly for TE purposes, as depicted in scheme 1. By following this strategy, modulated 3D structures have the option to change the cell microenvironment. The 3D constructs could be adapted from one having the solid or non-liquefied core fiber (scheme 1(C)), which has a more rigid microenvironment, leading to reduce cell mobility, or from the other with a liquefied core (scheme 1(D)) with increased cell mobility. Optical pictures clearly support our idea of using cell-laden fibers to produce the desired liquefied 3D construct (figure 3). The aforementioned observations made for the cell-free constructs seem to be also replicated in the case of the cell-laden constructs. Overall, this whole arrangement resembles a change in configuration of encapsulated cells from a planar level (fiber, horizontal) to a spiral position (vertical) held by a polyelectrolyte membrane. The diffusion properties of the 3D systems might be modulated by controlling the properties of the multilayered coatings, reported as permselective, which is an important feature to be considered regarding nutrients and metabolic wastes exchange. Additionally, the liquefied microenvironment can also be tailored to address different TE requirements by combining other polymers or bioactive molecules in fibers or other building blocks.

In order to assess whether processing the cell-laden structures by this methodology could be harsh for the cells, simple alginate fibers along with both types of 3D spiral constructs were also cultured over 7 d and assessed for viability, metabolic activity, and dsDNA content (figure 4).

After 7 d in culture, few dead (red) cells could be observed in all the conditions, thus suggesting the cell-

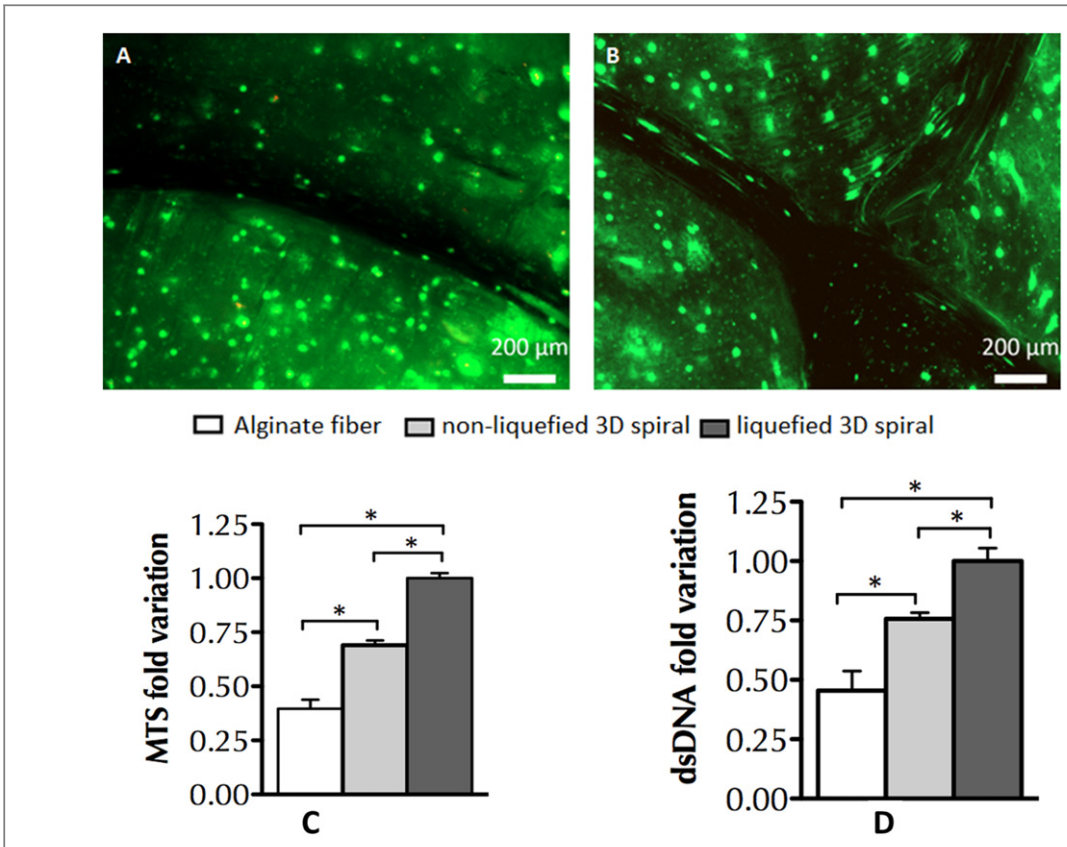

Figure 4. Cell behavior assessment onto the 3D spiral constructs using L929 cell viability at 7 d of culture. (A) LIVE/DEAD fluorescence assay at day 7 of cell culture of non-liquefied and (B) liquefied 3D constructs. Living cells were stained green by calcein-AM and dead cells red by propidium iodide. (C) MTS colorimetric assay of Ca-Alg fibers, non-liquefied and liquefied 3D spiral constructs after 7 d of culture. (D) dsDNA fold increase of L929 after 7 d in cultures. All statistical significances are indicated with *. ($p < 0.05, 24 > n > 3$).

friendly nature of the technique herein proposed to produce such 3D constructs (figures 4(A) and (B)). This was ably supported by observing total metabolic activity and dsDNA content. The values obtained for the spiral structures varied significantly, depending on the presence of LbL coating or whether the core was liquefied. The following trend was observed: alginate fiber < non-liquefied < liquified 3D spiral constructs. Although no other time-points were performed, one can consider that the increase in dsDNA content is indicative of an increase in cell proliferation. The liquefied environment of the constructs was more suitable for cell proliferation than the non-liquefied one, which could be due to the increased diffusion. These results further indicate that the perfusion-based LbL technique can be performed in cell-laden, shaped hydrogels without affecting the cell viability or the proliferative potential.

4. Conclusions

In this work, we have shown for the first time that cell-encapsulated fibers, behaving as building blocks, were molded to centimeter-long, spiral-shaped constructs and stabilized by using the perfusion-based LbL method. This bottom-up methodology aimed to provide a new method to control the size, shape, and other features of cell-laden, fiber-based constructs for TE applications. These assemblies displayed macroscopic benefits, such as structural flexibility and shape adjustability. The whole 3D construct performed as a distinct compartment where the cell microenvironment can be altered. With this platform technology, we can select cell types that can be used at different processing stages of a 3D construct, based on both rigid and liquefied internal microenvironments. This method may be further improved by customizing the selected biomaterials to mimic the natural extracellular matrix within the liquefied space and by combining different cell types. Although the construct remained stable during all the experimental work, a more systemic study is needed in order to comment on the long-time stability of the construct. In the future, fibers with different diameters may be used as building blocks by modifying the extrusion and ionotropic gelation conditions of Alg. The selection of different materials for the LbL coating may lead to the development of structures exhibiting selective permeability and the propensity to modulate the cell behavior. We foresee that such simple technologies can provide versatile hydrogel-based 3D constructs, which could lead to the formation of complex tissue and organ substitutes for TE applications.

Acknowledgments

The authors acknowledge the financial support by the Portuguese Foundation for Science and Technology (FCT) for grants SFRH/BPD/48948/2008, SFRH/BD/70107/2010 and project PTDC/CTM-BIO/1814/2012. This work has also received funding from the European Union's 7th framework program (FP7/2007–2013) under grant agreement no REGPOT-CT2012-316331-POLARIS and also from FEDER through the competitive factors operation program (COMPETE).

References

[1] Leferink A, Schipper D, Arts E, Vrij E, Rivron N, Karperien M, Mittmann K, van Blitterswijk C, Moroni L and Truckenmüller R 2014 Engineered micro-objects as scaffolding elements in cellular building blocks for bottom-up tissue engineering *Adv. Mater.* **26** 2592–9

[2] Zorlutuna P, Vrana N E and Khademhosseini A 2013 The expanding world of tissue engineering: new building blocks and applications of tissue engineered constructs *IEEE Rev. Biomed. Eng.* **6** 47–62

[3] Villar G, Graham A D and Bayley H 2013 A tissue-like printed material *Science* **340** 48–52

[4] Eng G, Lee B W, Parsa H, Chin C D, Schneider J, Linkov G, Sia S K and Vunjak-Novakovic G 2013 Assembly of complex cell microenvironments using geometrically docked hydrogel shapes *Proc. Natl. Acad. Sci. USA* **110** 4551–6

[5] Schober A, Fernekorn U, Singh S, Schlingloff G, Gebinoga M, Hampl J and Williamson A 2013 Mimicking the biological world: methods for the 3D structuring of artificial cellular environments *Eng. Life Sci.* **13** 352–67

[6] Tseng P, Kunze A, Kittur H and Di Carlo D 2014 Research highlights: microtechnologies for engineering the cellular environment *Lab. Chip.* **14** 1226–9

[7] Yan J, Huang Y and Chrisey D B 2013 Laser-assisted printing of alginate long tubes and annular constructs *Biofabrication* **5** 015002

[8] Lee B R, Lee K H, Kang E, Kim D S and Lee S H 2011 Microfluidic wet spinning of chitosan-alginate microfibers and encapsulation of HepG2 cells in fibers *Biomicrofluidics* **5** 022208

[9] Su J, Zheng Y and Wu H 2009 Generation of alginate microfibers with a roller-assisted microfluidic system *Lab. Chip.* **9** 996–1001

[10] Onoe H *et al* 2013 Metre-long cell-laden microfibres exhibit tissue morphologies and functions *Nat. Mater.* **12** 584–90

[11] Kiriya D, Ikeda M, Onoe H, Takinoue M, Komatsu H, Shimoyama Y, Hamachi I and Takeuchi S 2012 Meter-long and robust supramolecular strands encapsulated in hydrogel jackets *Angew. Chem. Int. Ed.* **51** 1553–7

[12] Tamayol A, Akbari M, Annabi N, Paul A, Khademhosseini A and Juncker D 2013 Fiber-based tissue engineering: progress, challenges, and opportunities *Biotechnol. Adv.* **31** 669–87

[13] Jun Y, Kang E, Chae S and Lee S H 2014 Microfluidic spinning of micro- and nano-scale fibers for tissue engineering *Lab. Chip.* **14** 2145–60

[14] Zhang S *et al* 2014 Creating polymer hydrogel microfibres with internal alignment via electrical and mechanical stretching *Biomaterials* **35** 3243–51

[15] Shin S J, Park J Y, Lee J Y, Park H, Park Y D, Lee K B, Whang C M and Lee S H 2007 'On the fly' continuous generation of alginate fibers using a microfluidic device *Langmuir* **23** 9104–8

[16] Sugiura S, Oda T, Aoyagi Y, Satake M, Ohkohchi N and Nakajima M 2008 Tubular gel fabrication and cell encapsulation in laminar flow stream formed by microfabricated nozzle array *Lab. Chip.* **8** 1255–7

[17] Liberski A R, Delaney J T, Schäfer H, Perelaer J and Schubert U S 2011 Organ weaving: woven threads and sheets as a step towards a new strategy for artificial organ development *Macromol. Biosci.* **11** 1491–8

[18] Hu M, Deng R, Schumacher K M, Kurisawa M, Ye H, Purnamawati K and Ying J Y 2010 Hydrodynamic spinning of hydrogel fibers *Biomaterials* **31** 863–9

[19] Jakab K, Norotte C, Marga F, Murphy K, Vunjak-Novakovic G and Forgacs G 2010 Tissue engineering by self-assembly and bio-printing of living cells *Biofabrication* **2** 022001

[20] Bertassoni L E *et al* 2014 Direct-write bioprinting of cell-laden methacrylated gelatin hydrogels *Biofabrication* **6** 024105

[21] Murphy S V and Atala A 2014 3D bioprinting of tissues and organs *Nat. Biotechnol.* **32** 773–85

[22] Lin H, Zhang D, Alexander P G, Yang G, Tan J, Cheng A W M and Tuan R S 2013 Application of visible light-based projection stereolithography for live cell-scaffold fabrication with designed architecture *Biomaterials* **34** 331–9

[23] Van Tomme S R, Storm G and Hennink W E 2008 *In situ* gelling hydrogels for pharmaceutical and biomedical applications *Int. J. Pharm.* **355** 1–18

[24] Lenas P, Luyten F P, Doblare M, Nicodemou-Lena E and Lanzara A E 2011 Modularity in developmental biology and artificial organs: a missing concept in tissue engineering *Artif. Organs* **35** 656–62

[25] Dixon J E, Shah D A, Rogers C, Hall S, Weston N, Parmenter C D J, McNally D, Denning C and Shakesheff K M 2014 Combined hydrogels that switch human pluripotent stem cells from self-renewal to differentiation *Proc. Natl. Acad. Sci. USA* **111** 5580–5

[26] Augst A D, Kong H J and mooney D J 2006 Alginate hydrogels as biomaterials *Macromol. Biosci.* **6** 623–33

[27] Lee B B, Ravindra P and Chan E S 2013 Size and shape of calcium alginate beads produced by extrusion dripping *Chem. Eng. Technol.* **36** 1627–42

[28] Orive G *et al* 2003 Cell encapsulation: promise and progress *Nat. Med.* **9** 104–7

[29] Sher P, Custódio C A and Mano J F 2010 Layer-by-layer technique for producing porous nanostructured 3D constructs using moldable freeform assembly of spherical templates *Small* **6** 2644–8

[30] Sher P and Mano J F 2012 Multilayers as 3D nanostructured porous constructs *Bioinspired, Biomim. Nanobiomaterials* **1** 245–51

[31] Silva J M, Georgi N, Costa R, Sher P, Reis R L, Van Blitterswijk C A, Karperien M and Mano J F 2013 Nanostructured 3D constructs based on chitosan and chondroitin sulphate multilayers for cartilage tissue engineering *PLoS ONE* **8** e55451

[32] Costa N L, Sher P and Mano J F 2011 Liquefied capsules coated with multilayered polyelectrolyte films for cell immobilization *Adv. Eng. Mater.* **13** B218–24

[33] Correia C R, Reis R L and Mano J F 2013 Multilayered hierarchical capsules providing cell adhesion sites *Biomacromolecules* **14** 743–51

[34] Correia C R, Sher P, Reis R L and Mano J F 2013 Liquified chitosan–alginate multilayer capsules incorporating poly(L-lactic acid) microparticles as cell carriers *Soft Matter* **9** 2125–30

[35] Costa R R and Mano J F 2014 Polyelectrolyte multilayered assemblies in biomedical technologies *Chem. Soc. Rev.* **43** 3453–79

[36] Borges J and Mano J F 2014 Molecular interactions driving the layer-by-layer assembly of multilayers *Chem. Rev.* **114** 8883–942